ELSEVIER

Applied Catalysis A: General 219 (2001) 53–60

APPLIED CATALYSIS A: GENERAL

www.elsevier.com/locate/apcata

An XPS study of La_2O_3 and In_2O_3 influence on the physicochemical properties of MoO_3/TiO_2 catalysts

Benjaram M. Reddy [a,*], Biswajit Chowdhury [a], Panagiotis G. Smirniotis [b,1]

[a] *Inorganic and Physical Chemistry Division, Indian Institute of Chemical Technology, Hyderabad 500007, Andhra Pradesh, India*
[b] *Chemical Engineering Department, University of Cincinnati, Cincinnati, OH 45221-0171, USA*

Received 6 March 2001; received in revised form 16 May 2001; accepted 18 May 2001

Abstract

To explore the influence of La_2O_3 and In_2O_3 doped TiO_2 support on the dispersion and chemical nature of Mo-oxide species an investigation was undertaken by using XPS and other techniques. In this study, the La_2O_3–TiO_2 and the In_2O_3–TiO_2 binary oxide supports were prepared by a homogeneous coprecipitation method with in situ generated ammonium hydroxide and were deposited with MoO_3 by adopting a wet impregnation technique. The Mo-containing catalysts and the corresponding supports were characterized by means of XRD, FTIR, XPS, and BET surface area methods. Characterization results suggest that the calcined (773 K) La_2O_3–TiO_2 and In_2O_3–TiO_2 binary oxides are in X-ray amorphous state and exhibit reasonably high specific surface area. These supports also accommodate a monolayer equivalent of MoO_3 (12 wt.%) in a highly dispersed state on the surface. Both La_2O_3 and In_2O_3 dopants show a strong influence on the electronic properties of the MoO_3/TiO_2 catalysts as evidenced by a change in the XPS binding energies of these metal oxides. The XPS binding energy values further indicate that the dispersed molybdenum oxide is in Mo(VI) oxidation-state. However, the maximum broadening of Mo 3d as observed from full width at half-maximum values indicates that the presence of different Mo(VI) species on both the support surfaces.

Keywords: Molybdenum oxide; La_2O_3–TiO_2; In_2O_3–TiO_2; Mixed oxide; Acid–base properties; X-ray diffraction; X-ray photoelectron spectroscopy; Dispersion

1. Introduction

Molybdena–titania catalysts are excellent for selective oxidation of hydrocarbons [1], ammoxidation of hetero-aromatic compounds [2], and selective catalytic reduction of NO_x with ammonia [3]. Moreover they are the precursors of alkene metathesis catalysts [4] and of sulfided hydrodesulfurization catalysts [5,6]. It is an established fact in the literature that the activity and selectivity of the supported molybdenum catalysts is highly sensitive to the composition of the support and in the case of TiO_2-supported catalysts, the phase of support [7]. Eon et al. [8] have suggested that molybdena–titania interaction takes place through a perfect adjustment of (0 1 0) planes of MoO_3 with (0 0 1) planes of TiO_2-anatase, thus leading to an epitaxial growth in the (0 1 0) direction of MoO_3 crystals over the TiO_2. A high dispersion of octahedral polymolybdate over titania surface was reported by Ng and Gulari [9] by using laser Raman and IR spectroscopic methods. Other investigators

* Corresponding author. Fax: +91-40-7173387.
E-mail addresses: bmreddy@iict.ap.nic.in (B.M. Reddy), panagiotis.smirniotis@uc.edu (P.G. Smirniotis).
[1] Co-corresponding author. Fax: +1-513-556-3473.

0926-860X/01/$ – see front matter
PII: S0926-860X(01)00658-5

employing ESR and other techniques have also supported these observations [10].

Oxidation reactions are playing an important role, both in the production of useful chemicals as well as in the destruction of undesired organics by total catalytic oxidation. Several efforts are being made in the literature on the one hand to develop various kinds of new catalysts to satisfy the needs for practical applications, and on the other hand, to explore the nature and structure of the active phase of the catalysts by employing several modern physicochemical techniques [11–14]. Recently, we have reported that the titania anatase structure can be stabilized even up to 1273 K with incorporation of other stable oxides such as Al_2O_3, SiO_2, and ZrO_2 and having vanadium or molybdenum oxides present as a monolayer on these mixed oxide surfaces [15–17]. In particular, the combined V_2O_5/Ga_2O_3–TiO_2 catalyst was found to exhibit interesting catalytic activity for the selective oxidation of 4-methylanisole to anisaldehyde [18]. The La_2O_3 is an important basic material and has been widely employed as a catalyst [19] and catalyst support [20], particularly in the oxidative coupling of methane (OCM). The lanthanum titanate catalyst activates methane more selectively than the individual oxides [19]. The In_2O_3 is another interesting basic oxide, which has also often been used as a promoter in HZSM-5 zeolites for SCR of NO with CH_4 in the presence of excess oxygen [21].

Over the past years, a great deal of fundamental and applied research work was focussed, especially, on supported molybdena catalysts because of their numerous applications in petroleum refining, chemicals production, and pollution control industries [1,5,9,11–15]. The Mo-oxide catalysts supported on conventional supports such as Al_2O_3, SiO_2 and TiO_2 have been extensively investigated by a variety of techniques, conventional bulk sampling techniques as well as surface sensitive electron and ion spectroscopies, in an attempt to elucidate the nature of catalytic active surface species, and to study the coordination environment of the active metal center. The high surface sensitive photoelectron spectroscopy (XPS), is one of the best techniques to study the nature of Mo-oxide species on different supports.

In continuation to our earlier effort of making various kinds of mixed oxides possessing different acid–base characteristics [17,22], in this study, the La_2O_3–TiO_2 and the In_2O_3–TiO_2 binary oxides have been prepared, deposited with MoO_3 by adopting a wet impregnation technique, and were investigated by XPS and other techniques. The primary goal of this study was to explore the influence of the surface structure of the support on the dispersion and chemical nature of Mo-oxide species.

2. Experimental methods

2.1. Catalyst preparation

The La_2O_3–TiO_2 (1:5 molar ratio) and In_2O_3–TiO_2 (1:13 molar ratio) binary oxides were prepared by a co-precipitation method where ammonia was generated in situ by decomposition of urea at 363 K [23]. In a typical experiment, the required quantities of titanium tetrachloride (Fluka, AR grade) and lanthanum nitrate (Loba, GR grade) or indium chloride (Aldrich, AR grade), dissolved separately in deionized water were mixed together. Cold $TiCl_4$ was first digested in cold concentrated HCl and subsequently diluted with deionized water. In the case of In_2O_3–TiO_2 mixed oxide, the indium chloride precursor was dissolved in an excess solution of ethanol. An excess amount of solid urea with a metal to urea molar ratio of 1:2.5 was also added to the mixture solution. The resulting mixture was heated slowly to 363–368 K on a hot plate with vigorous stirring. The pH of the solution was monitored at different intervals of time. No change in the pH of the solution was observed until the temperature reached to 363–368 K. At this temperature the pH of the solution increased slowly in the beginning from 3.5 to 4.5 and rapidly with increase in the time of heating, attaining a final value between 7 and 8. Heating was further continued at this temperature for 6 h in order to complete the precipitation. The resulting precipitates were filtered, washed with deionized water until no chlorides could be detected with $AgNO_3$ in the filtrate. The resulting cake was then oven dried at 383 K for 12 h and finally calcined at 773 K for 6 h in air atmosphere. A nominal 12 wt.% MoO_3 was deposited on the calcined mixed oxides by adopting a wet impregnation method [15]. To impregnate MoO_3 the calculated amount of ammonium heptamolybdate (J.T. Baker, UK, AR grade) was dissolved in doubly distilled water and a few drops of dilute NH_4OH was

added to make the solution clear and to keep the pH constant (pH 8). Finely powdered calcined (773 K) supports were then added to this solution and the excess water was evaporated on a water-bath with continuous stirring. The resultant solid was then dried at 383 K for 12 h and calcined at 773 K for 5 h in the flow of oxygen (40 $cm^3\ min^{-1}$). The rate of heating (as well as cooling) was always maintained at 10 $K\ min^{-1}$.

2.2. Catalyst characterization

X-ray diffraction analysis was performed on a Siemens D-5000 diffractometer by using Cu Kα radiation source and Scintillation Counter detector. The XRD phases present in the samples were identified with the help of ASTM Powder Data Files. The BET surface area of the samples was determined by N_2 physisorption at 77 K by taking 0.162 nm^2 as the area of cross section of N_2 molecule.

The XPS measurements were made on a VG scientific ESCA Lab II Spectrometer (resolution 0.1 eV) with Mg Kα (1253.6 eV) radiation as the excitation source [16]. Before experiments the spectrometer was calibrated against Eb(Au $4f_{7/2}$) = 84.0 eV and Eb(Cu $2p_{3/2}$) = 932.6 eV [24]. The C 1s line was taken as internal reference with a binding energy of 285.0 eV [24]. An estimated error of +0.1 eV can be assumed for all the measurements. The finely ground oven dried samples were mounted on the standard sample holder and covered by a gold mask. The sample holder was then fixed on a rod attached to the pretreatment chamber. Before transferring them to the main chamber the samples were degassed (1×10^{-7} Torr) in the pretreatment chamber overnight at room temperature. The degassed samples were then transferred into the main chamber and the XPS analysis was done at room temperature and pressures typically less than 10^{-8} Torr [24].

3. Results and discussion

X-ray powder diffraction patterns of La_2O_3–TiO_2 and In_2O_3–TiO_2 supports along with their corresponding MoO_3 containing catalysts are shown in Fig. 1. As can be noted, the lanthana–titania binary oxide is in X-ray amorphous state with broad background diffraction lines due to a poorly crystalline TiO_2 anatase phase (JCPDS Files no. 21-1272). However, in the case of In_2O_3–TiO_2 sample, a few characteristic TiO_2-anatase lines can be seen indicating that this material is in a slightly crystalline form than that of La_2O_3–TiO_2. It can also be noted from Fig. 1 that in both the cases that there is no evidence of any specific compound formation between La_2O_3 or In_2O_3 and TiO_2. The FTIR spectra of these samples also supported the XRD observations indicating that there is no evidence of the formation of oxide compounds of lanthanum or indium with titanium when calcined at 773 K. The MoO_3/La_2O_3–TiO_2 is also in X-ray amorphous state with broad background lines due to TiO_2-anatase phase, whereas the MoO_3/In_2O_3–TiO_2 catalyst exhibits a few characteristic TiO_2-anatase lines. Very interestingly, no XRD lines due to crystalline MoO_3 or TiO_2-rutile phases were observed in both cases. This observation indicates that the impregnated molybdenum oxide is in a highly dispersed state or the crystallites formed are less than the detection capability of the XRD technique. The 12 wt.% loading of MoO_3 corresponds to the monolayer capacities of these oxides and supports the former possibility [25]. The FTIR spectra of these samples also supported the XRD observations. Anatase phase of titania normally exhibits strong absorption bands at 676 and 547 cm^{-1} and the rutile phase at 660 and 455 cm^{-1}, respectively [26]. The presence of these bands due to TiO_2-anatase phase is noted for both series of samples. Generally, the IR band of Mo=O in crystalline MoO_3 appears at 1000 cm^{-1} due to the stretching vibration mode [15,26,27]. Irrespective of the support, no characteristic bands due to crystalline MoO_3 were observed which indicates clearly that the molybdenum oxide is in a highly dispersed state on the support. As shown in Table 1, both supports show reasonably high specific surface areas. After impregnation with MoO_3 a small decrease in the specific surface area of the samples can be noted. This is primarily due to a high dispersion of molybdenum oxide in the pores of the support [15]. The O_2 chemisorption measurements as per the procedure described elsewhere [15] also reveal that the impregnated molybdenum oxide is in a highly dispersed state on both support surfaces. This method nicely discriminates between the dispersed state and the crystalline molybdenum oxide phase.

The La_2O_3–TiO_2, In_2O_3–TiO_2, MoO_3/La_2O_3–TiO_2 and MoO_3/In_2O_3–TiO_2 samples were investigated by

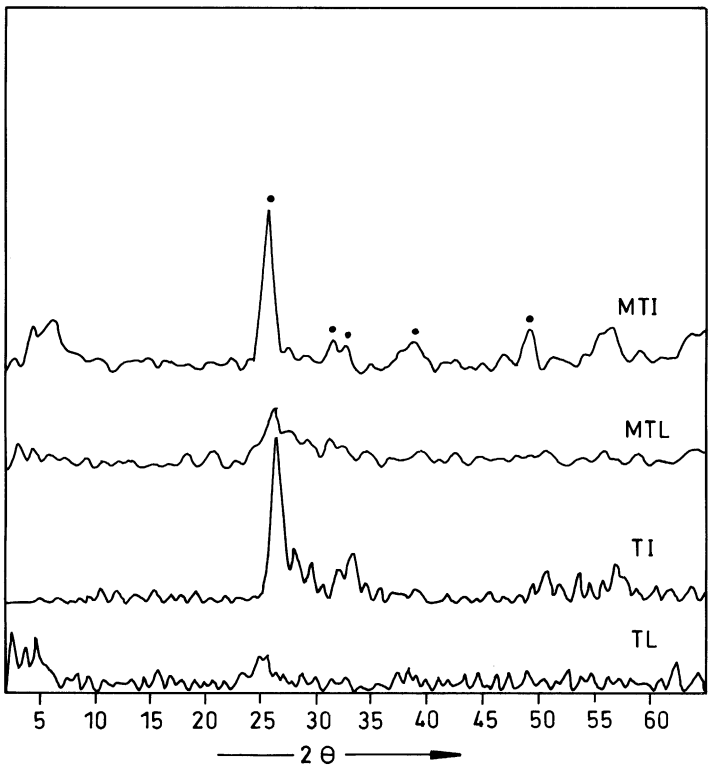

Fig. 1. X-ray powder diffraction patterns of La_2O_3–TiO_2, In_2O_3–TiO_2, MoO_3/La_2O_3–TiO_2 and MoO_3/In_2O_3–TiO_2 samples calcined at 773 K. (●) Lines due to TiO_2-anatase phase.

Table 1
Composition, BET surface area and XRD phase composition of the samples investigated in this study

Sample	Support composition (mole ratio)	BET SA ($m^2\,g^{-1}$)	XRD phases observed
La_2O_3–TiO_2	1:5	132	Amorphous
In_2O_3–TiO_2	1:13	125	TiO_2-anatase
MoO_3/La_2O_3–TiO_2	1:5	96	Amorphous
MoO_3/In_2O_3–TiO_2	1:13	115	TiO_2-anatase

XPS technique. The representative XPS bands of O 1s, Ti 2p together with In 3d, La 3d, and Mo 3d without smoothing are shown in Figs. 2–5, respectively, and the corresponding binding energies and full width at half maximum (FWHM) values are summarized in Table 2. For the purpose of better comparison, the XPS bands of O 1s and Ti 2p along with In 3d pertaining to the supports are shown in Figs. 2a and 3a, respectively, and the corresponding bands of MoO_3 containing catalysts are shown in Figs. 2b and 3b, respectively. These figures and Table 2 clearly indicate that the XPS bands are highly sensitive to the composition of the mixed oxide support and also the presence of MoO_3 on these carriers.

The O 1s profile, as presented in Fig. 2, is complicated due to the overlapping contribution of oxygen from both individual oxides as well as from MoO_3 in the case of Mo-containing catalysts. As reported in the literature [24,28], the O 1s binding energy of pure TiO_2 is 530.1 eV. However, a small lowering of the

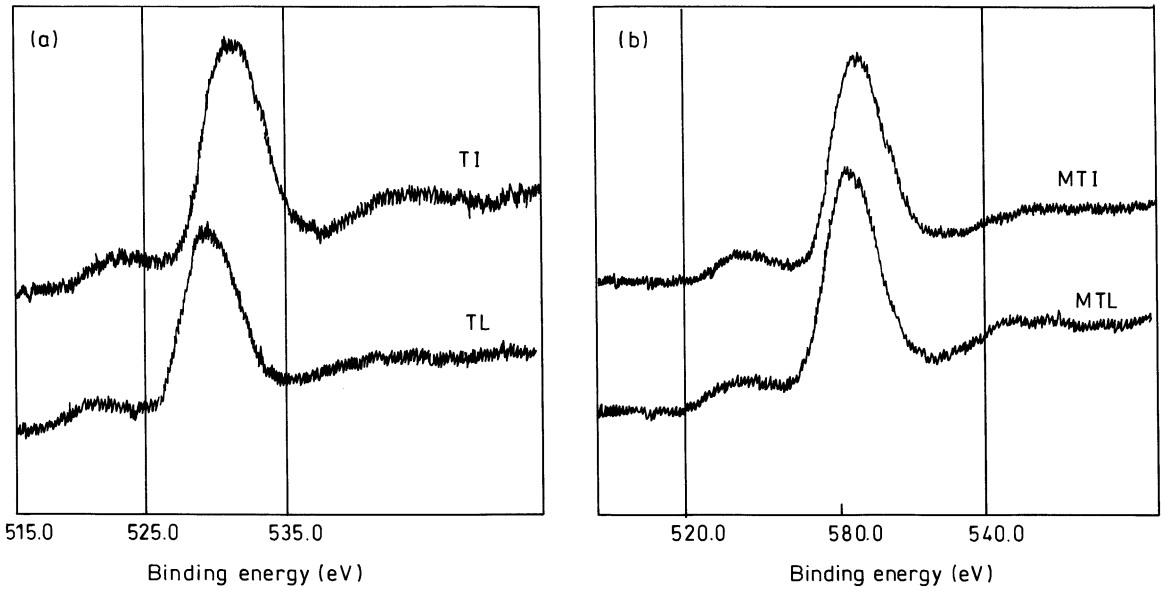

Fig. 2. XPS of the O 1s region for La_2O_3–TiO_2, In_2O_3–TiO_2, MoO_3/La_2O_3–TiO_2 and MoO_3/In_2O_3–TiO_2 samples calcined at 773 K.

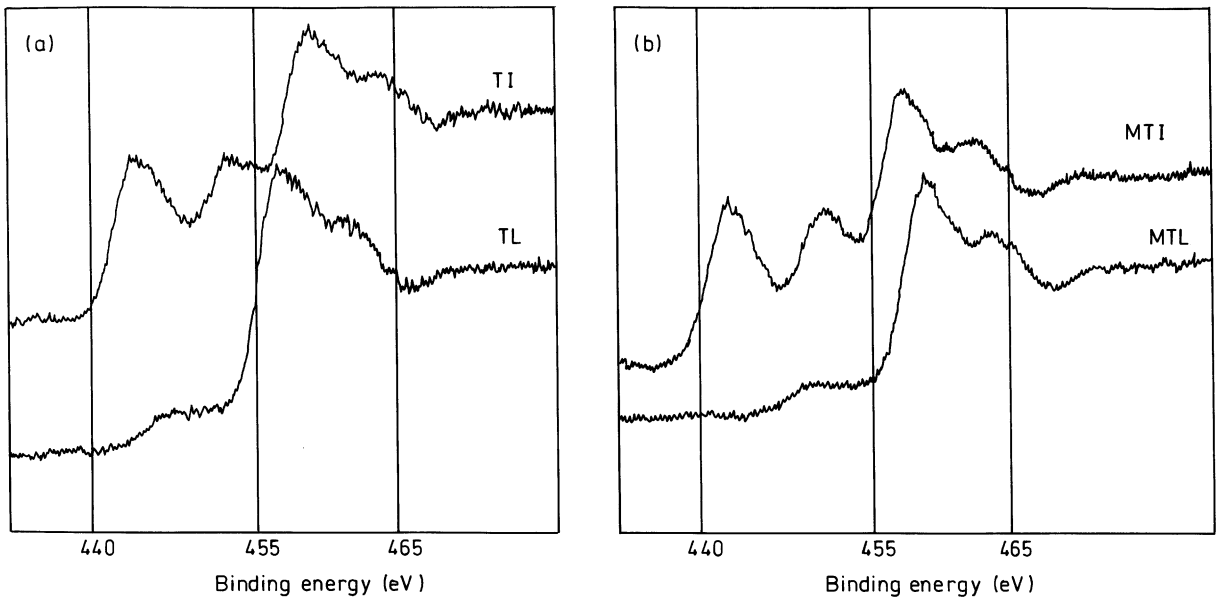

Fig. 3. (a) Ti 2p and In 3d XPS binding energy region for La_2O_3–TiO_2 and In_2O_3–TiO_2 samples. (b) Ti 2p and In 3d XPS binding energy region for MoO_3/La_2O_3–TiO_2 and MoO_3/In_2O_3–TiO_2 samples.

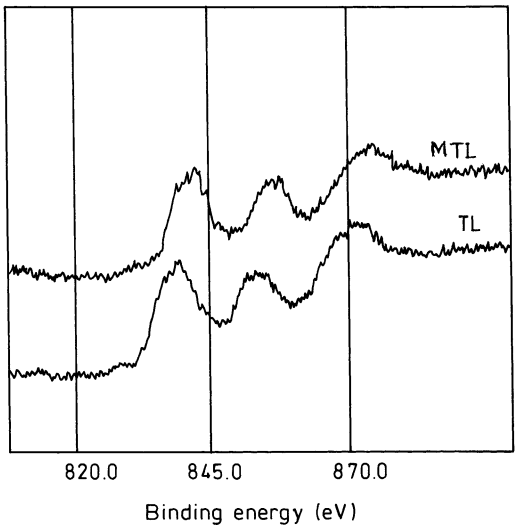

Fig. 4. La 3d XPS spectra of La_2O_3–TiO_2 and MoO_3/La_2O_3–TiO_2 samples calcined at 773 K.

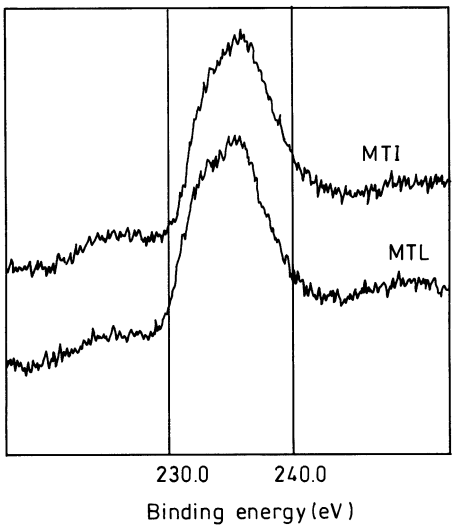

Fig. 5. Mo 3d XPS spectra of MoO_3/La_2O_3–TiO_2 and MoO_3/In_2O_3–TiO_2 samples calcined at 773 K.

O 1s binding energy can be noted for La_2O_3–TiO_2 sample as well as for Mo-containing catalysts.

Fig. 3 shows the binding energies of Ti 2p photoelectron peaks at around 458.0 and 464.0 eV for Ti $2p_{3/2}$ and Ti $2p_{1/2}$ lines, respectively. As In 3d core level binding energy value (444.6 eV for pure In_2O_3 [29]) is closer to Ti 2p binding energy values, therefore, both have been recorded in the same range and presented in Fig. 3. As shown in Table 2, the Ti $2p_{3/2}$ binding energy of the La_2O_3–TiO_2 mixed oxide was found to be 457.0 eV, which is lower than that of the pure TiO_2 (458.0 eV) [30]. The Pauling electronegativity value of Ti is 1.5 and of La is 1.1 [31], which indicates the possibility of electron transfer from lanthanum to titanium in the Ti–O–La bond. This charge transfer makes Ti more electron rich and lowers the Ti $2p_{3/2}$ core electron binding energy. Moreover, the binding energy value for La 3d also decreases for La_2O_3 in the mixed oxide as compared to the value found at 834.8 eV for pure lanthanum oxide [24]. In the case of In_2O_3–TiO_2 sample, the core level binding energy of Ti 2p was found to be 459.0 eV, which is more than that of pure titania. It can be interpreted again from the Pauling electronegativity values of the corresponding elements. Pauling E.N. value for indium is 1.7, which is more than that of titania thus favoring negative charge transfer towards indium in the Ti–O–In bond thereby increasing Ti 2p core level binding energy. The binding energy value of In 3d in the mixed oxide remains the same with that found in the literature [32,33] for pure indium oxide. Substitution of In^{3+} in the titania matrix generates an excess negative charge around these elements due to non-stoichiometric oxide ion. Therefore, the corresponding binding energy of In 3d remains the same in the mixed oxides.

Table 2
XPS binding energies and FWHM values of binary oxide supports and MoO_3 containing catalysts

Sample	O 1s (eV)	Ti $2p_{3/2}$ (eV)	La 3d (eV)	In 3d (eV)	Mo 3d (eV)	FWHM (eV)
La_2O_3–TiO_2	529.0	457.0	833.0	–	–	–
In_2O_3–TiO_2	530.0	459.0	–	444.5	–	–
MoO_3/La_2O_3–TiO_2	529.5	458.5	834.0	–	235.0	7.5
MoO_3/In_2O_3–TiO_2	529.5	457.5	–	443.0	234.0	8.0

The binding energy values of La 3d and In 3d for MoO_3/La_2O_3–TiO_2 and MoO_3/In_2O_3–TiO_2, respectively, was decreased when compared to the values found for the corresponding pure oxides [24,29]. The explanation is that because of strong interaction between the acidic MoO_3 and basic La_2O_3 and In_2O_3 oxides there is strong shift in the BE values of the corresponding oxides when compared to the pure supports. The same was also responsible for the broadening of Mo 3d line.

Fig. 4 presents the XPS patterns of La 3d levels before and after impregnating with MoO_3. Apart from La 3d doublet at around 834.8 eV, a third peak in the figure is due to the auger emission from titanium atom [34]. The Mo $3d_{5/2}$ photoelectron peak of MoO_3/La_2O_3–TiO_2 and MoO_3/In_2O_3–TiO_2 catalysts is shown in Fig. 5. The binding energy values presented in Table 2 indicate the presence of Mo(VI) species on both support surfaces [35]. The FWHM values shown in Table 2 indicate clearly the presence of different molybdena species on both support surfaces as envisaged earlier [22,36]. The Mo 3d doublet was well resolved in the case of MoO_3/TiO_2–ZrO_2 and MoO_3/TiO_2–SiO_2 samples and a maximum peak broadening was noted in the case of MoO_3/TiO_2–Al_2O_3 samples [22]. The literature reveals that the resolution of the doublet peak is quite poorer for MoO_3/Al_2O_3 catalyst and improves considerably as one passes from Mo/SiO_2 to Mo/ZrO_2 to Mo/TiO_2 systems [36]. The broadening of ESCA peak has been attributed to various factors including (1) the presence of more than one type of Mo(VI) with different chemical characteristics which cannot be discerned by ESCA [36,37], and (2) electron transfer between the active component and the support (metal–support interaction). At monolayer coverage the structure of surface molybdenum oxide species primarily possesses an octahedral coordination on TiO_2 and a mixture of tetrahedral and octahedral coordination on Al_2O_3 surface. A maximum Mo 3d peak broadening observed in the case of MoO_3/TiO_2–Al_2O_3 sample was attributed to the existence of different octahedral and tetrahedral Mo species on this mixed oxide surface. The same analogy can be extended to the present catalyst systems where a similar Mo 3d broadening is noted. In particular, the La_2O_3 and In_2O_3 oxides in TiO_2 show a strong influence on the chemical state of molybdenum when compared to other additives such as Al_2O_3, SiO_2 and ZrO_2. This is primarily due a strong acid–base interaction between the basic La_2O_3 and In_2O_3 oxides and the acidic MoO_3.

It is an established fact in the literature that the nature of the surface molybdenum oxide species formation in a supported catalyst system mainly depends (i) on the nature and number of OH groups present on the support; (ii) mode of binding of Mo oxide precursors to OH groups during impregnation; and (iii) transformation of surface species during drying and calcination. The NH_4^+ ions are removed during calcination and the H^+ ion coordinate to the surface molybdenum oxide species in order to compensate for the net charge. Therefore, the molecular structures of the surface molybdenum oxide species of the calcined samples are mainly dependent on the net surface pH at point of zero charge (PZC) [38]. The oxide supports with low pH at PZC such as SiO_2 (pH at PZC = 1.8–3.9) were found to favor the octahedrally coordinated polymolybdate species such as $Mo_8O_{26}^{4-}$ and/or $Mo_7O_{24}^{6-}$. On the other hand, the amphoteric oxide supports, TiO_2 (anatase, pH at PZC = 6.2) and ZrO_2 (pH at PZC = 6.7), favor the formation of same octahedrally coordinated polymolybdate species. The Al_2O_3 support (pH at PZC 6.0–8.9) possesses both monomeric (MoO_4^{2-}) and polymeric species ($Mo_7O_{24}^{6-}$) at high pH values. Presence of basic La_2O_3 and In_2O_3 oxides in the TiO_2 support is expected to increase its pH at PZC. Therefore, different surface molybdena species are expected to be formed in conformity with the XPS observations.

4. Conclusions

The following conclusions can be drawn from this study: (1) The La_2O_3–TiO_2 and In_2O_3–TiO_2 binary oxides are interesting and promising support materials for the dispersion of molybdenum oxide. These calcined (773 K) mixed oxides are in X-ray amorphous state with broad diffraction lines due TiO_2-anatase phase and exhibit a high specific surface area. (2) The MoO_3/La_2O_3–TiO_2 and MoO_3/In_2O_3–TiO_2 catalysts calcined at 773 K also retain the TiO_2-anatase phase of the support and the impregnated molybdenum oxide being in a highly dispersed state. (3) Both La_2O_3 and In_2O_3 dopants show a strong influence on the chemical

properties of the MoO_3/TiO_2 catalyst as evidenced by a change in the XPS binding energies. (4) The XPS binding energy values indicate that the dispersed molybdenum oxide is in Mo(VI) oxidation-state. However, the maximum broadening of Mo 3d as observed from FWHM values indicate the presence of different Mo(VI) species on both the supports.

Acknowledgements

B. Chowdhury is the recipient of senior research fellowship of the University Grants Commission, New Delhi.

References

[1] J. Haber, Role of Molybdenum in Catalysis, Climax Molybdenum Co., Ann Abor, MI, 1981.
[2] B.M. Reddy, B. Manohar, Chem. Ind. (London) (1992) 182.
[3] S. Okazaki, M. Kumasaka, J. Yoshida, K. Kosaka, K. Tanabe, Ind. Eng. Chem. Prod. Res. Div. 20 (1981) 301.
[4] K. Tanaka, K.I. Tanaka, J. Chem. Soc. Chem. Commun. (1984) 748.
[5] K. Segawa, T. Soeya, D.S. Kim, Res. Chem. Intermed. 15 (1991) 129.
[6] W. Zhaobin, X. Qin, G. Xiexian, P. Grange, B. Delmon, Appl. Catal. 75 (1991) 179.
[7] E. Bordes, S.J. Jung, P. Courtine, in: M.F. Portela (Ed.), Proceedings of the 9th Iberoamerican Symposium on Catalysis, Lisbon, 1984, p. 983.
[8] J.G. Eon, E. Bordes, A. Vejux, P. Courtine, in: K. Dyrek, J. Haber, J. Nowtony (Eds.), Proceedings of the Ninth Symposium on the Reactivity of Solids, PWN, Warnzac, 1982, p. 603.
[9] K.Y.S. Ng, E.J. Gulari, J. Catal. 92 (1985) 340.
[10] C.V. Caceres, J.L.G. Fierro, J. Lazaro, A.L. Agudo, J. Soria, J. Catal. 122 (1990) 113.
[11] K. Segawa, I.E. Wachs, in: I.E. Wachs (Ed.), Chracterization of Catalytic Materials, Butterworths, Heinemann, Boston, 1992, p. 72.
[12] D.M. Hercules, J.C. Klein, in: H. Windawi, F.F.L. Ho (Eds.), Applied Electron Spectroscopy for Chemical Analysis, Wiley, New York, 1982.
[13] H. Topsoe, in: J.P. Bonnelle, B. Delmon, E. Derouane (Eds.), Surface Properties and Catalysis by Non-Metals, Reidel, 1983, p. 329.
[14] H. Knözinger, in: M.J. Phillips, M. Ternan (Eds.), Proceedings of the 9th International Congress on Catalysis, Vol. 5, Calgary, 1988, The Chemical Society of Canada, Ottawa, 1989, p. 20.
[15] B.M. Reddy, B. Chowdhury, J. Catal. 179 (1998) 413.
[16] B.M. Reddy, I. Ganesh, E.P. Reddy, J. Phys. Chem. B 101 (1997) 1769.
[17] B.M. Reddy, I. Ganesh, B. Chowdhury, Catal. Today 49 (1999) 115, and references therein.
[18] B.M. Reddy, I. Ganesh, B. Chowdhury, Chem. Lett. (1997) 1145.
[19] H. Borchert, M. Baerns, J. Catal. 168 (1997) 315.
[20] A. Slagtern, Y. Schuurman, C. Leclercq, X. Verykios, C. Mirodatos, J. Catal. 172 (1997) 118.
[21] E. Kikuchi, K. Yogo, Catal. Today 22 (1994) 73.
[22] B.M. Reddy, B. Chowdhury, P.G. Smirniotis, Appl. Catal. A: Gen. 211 (2001) 19.
[23] B.M. Reddy, B. Manohar, S. Mehdi, J. Solid State Chem. 97 (1992) 317.
[24] D. Briggs, M.P. Seah (Eds.), Practical Surface Analysis, Auger and X-ray Photoelectron Spectroscopy, Vol. 1, 2nd Edition, Wiley, New York, 1990.
[25] A.J. van Hengstun, J.G. van Ommen, H. Bosch, P.J. Gellings, Appl. Catal. 5 (1983) 207.
[26] R.A. Nyquist, L.L. Putzig, M.A. Leugers, Handbook of Infrared and Raman Spectra of Inorganic Compounds and Organic Salts, Academic Press, New York, 1997.
[27] T. Frausen, P.C. van Berge, P. Mars, Preparation of Catalysts I, Elsevier, Amsterdam, 1976, p. 405.
[28] R. Castillo, B. Koch, P. Ruiz, B. Delmon, J. Catal. 161 (1996) 524.
[29] P.A. Bertrand, J. Vac. Sci. Technol. 18 (1981) 28.
[30] P. Wauthoz, M. Ruwet, T. Machej, P. Grange, Appl. Catal. 69 (1991) 149.
[31] J.D. Lee, Concise Inorganic Chemistry, 4th Edition, p. 160.
[32] L.P. Hack, J.E. de Vries, K.S Chattha F M.S. Otto, Appl. Catal. 82 (1992) 199.
[33] V. Parvulescu, S. Coman, V.I. Parvulescu, P. Grange, G. Poncelet, J. Catal. 180 (1998) 66.
[34] Y. Uwamino, Y. Ishizuka, H. Yamatera, J. Electron. Spectrosc. Related Phenom. 34 (1984) 69.
[35] T.A. Patterson, J.C. Carver, D.E. Leyden, D.M. Hercules, J. Phys. Chem. 80 (1976) 1700.
[36] N.K. Nag, J. Phys. Chem. 91 (1987) 2324, and references therein.
[37] P. Ratnasamy, J. Catal. 40 (1975) 137.
[38] G. Deo, I.E. Wachs, J. Phys. Chem. 95 (1991) 5889.